Dedifferentiation of Prostate Smooth Muscle Cells in Response to Bacterial LPS

Carolina Leimgruber,[1] Amado A. Quintar,[1] Liliana D.V. Sosa,[1] Luciana N. García,[1] Mauricio Figueredo,[2] and Cristina A. Maldonado[1]*

[1]*Center of Electron Microscopy, School of Medical Sciences, National University of Cordoba, Cordoba, Argentina*
[2]*CIBICI-CONICET, Department of Clinical Biochemistry, School of Chemical Sciences, National University of Cordoba, Cordoba, Argentina*

BACKGROUND. Prostate smooth muscle cells (SMCs) are strongly involved in the development and progression of benign prostatic hyperplasia and prostate cancer. However, their participation in prostatitis has not been completely elucidated. Thus, we aimed to characterize the response of normal SMC to bacterial lipopolysaccharide (LPS).
METHODS. Primary prostate SMCs from normal rats were stimulated with LPS (0.1, 1, or 10 μg/ml) for 24 or 48 hr. The phenotype was evaluated by electron microscopy, immunofluorescence, and Western blot of SMCα-actin (ACTA2), calponin, vimentin, and tenascin-C, while the innate immune response was assessed by immunodetection of TLR4, CD14, and nuclear NF-κB. The secretion of TNFα and IL6 was determined using ELISA.
RESULTS. Bacterial LPS induces SMCs to develop a secretory phenotype including dilated rough endoplasmic reticulum cisternae with well-developed Golgi complexes. Furthermore, SMCs displayed a decrease in ACTA2 and calponin, and an increase in vimentin levels after LPS challenge. The co-expression of ACTA2 and vimentin, together with the induction of tenascin-C expression indicate that a myofibroblastic-like phenotype was induced by the endotoxin. Moreover, LPS elicited a TLR4 increase, with a peak in NF-κB activation occurring after 10 min of treatment. Finally, LPS stimulated the secretion of IL6 and TNFα.
CONCLUSIONS. Prostate SMCs are capable of responding to LPS in vitro by dedifferentiating from a contractile to a miofibroblastic-like phenotype and secreting cytokines, with the TLR4 signaling pathway being involved in this response. In this way, prostate SMCs may contribute to the pathophysiology of inflammatory diseases by modifying the epithelial–stromal interactions. *Prostate 71: 1097–1107, 2011.* © 2010 Wiley-Liss, Inc.

KEY WORDS: **smooth muscle cells; dedifferentiation; LPS; innate immune response**

INTRODUCTION

The stromal compartment of the prostate is mainly comprised of smooth muscle cells (SMCs) and fibroblasts, with endothelial, macrophage, and other immune cells also occurring at lower quantities in the rat [1]. SMCs play a central role in the regulation of prostatic growth and function by secreting growth factors that inhibit excessive epithelial proliferation, thus participating in paracrine stromal–epithelial interactions in the gland [2,3]. Therefore, the maintenance of the SMC phenotype is critical in order to conserve the normal rate of cellular proliferation/death within the gland.

Grant sponsor: Consejo Nacional de Investigaciones Científicas y Técnicas (CONICET); Grant sponsor: FONCYT-ANPCyT (PICT 533).
*Correspondence to: Dr. Cristina A. Maldonado, Centro de Microscopía Electrónica, Facultad de Ciencias Médicas, Universidad Nacional de Córdoba, Pab. Biología Celular 1° piso, Haya de la Torre esq. Enrique Barros, Ciudad Universitaria, X5000HRA Córdoba, Argentina.
E-mail: cmaldon@cmefcm.uncor.edu
Received 15 November 2010; Accepted 23 November 2010
DOI 10.1002/pros.21322
Published online 28 December 2010 in Wiley Online Library (wileyonlinelibrary.com).

In recent years, the interest in prostatic SMCs has increased since they have been shown to be involved in all prostate pathologies, including prostatitis, benign prostatic hyperplasia (BPH), and prostate cancer, with these cells exhibiting changes in their number and phenotype. For instance, BPH, the most common non-malignant proliferative disorder in males, is considered to be primarily a stromal process characterized by the increase of alpha smooth muscle actin (ACTA2)-positive cells, which probably occurs due to proliferation and miodifferentiation of the stromal cells contributing to urethral obstruction [4–6]. Moreover, stromal cells can actively participate in the molecular mechanisms of BPH by secreting numerous proinflammatory cytokines and chemokines, thereby recruiting immune cells to the prostate with IL-8 subsequently inducing autocrine/paracrine proliferation of BPH cells [7].

In prostate cancer, the presence of dedifferentiated SMCs is a constant feature of the reactive stroma accompanying tumoral cells and is associated to carcinogenesis [8,9]. This reactive stroma leads to a significant decrease or even complete loss of fully differentiated SMCs, which are replaced by fibroblasts and myofibroblasts [9]. The myofibroblastic phenotype is considered to be an intermediate type between fibroblasts and SMC [10], and plays a fundamental role in the promotion, progression, and metastasis of prostate cancer [11].

Although the contribution of prostate SMCs in BPH and cancer has been extensively studied, their participation in prostatitis has not been complete elucidated. A few studies have concentrated on the effects of inflammation on the prostatic gland and have mostly been focused on evaluating epithelial aspects [12,13], but little information is available about the response of SMCs to infection or inflammation within the gland. However, for other inflammatory diseases such as asthma and atherosclerosis it is well-known that SMCs have a pivotal role in the pathogenesis [14,15]. Many works have reported that vascular SMCs alter their phenotype from a contractile to a secretory state during atherosclerosis [16]. Moreover, SMCs are capable of secreting proinflammatory cytokines, chemokines, and growth factors, thereby contributing to the inflammatory microenvironment in several organs and diseases [17].

We have previously reported that acute bacterial infection induces an initial hypertrophy of rat periacinar prostate SMCs, before later acquiring a secretory phenotype, with a reduction of ACTA2 at 72-hr post-infection [18]. As part of this reaction, prostatic SMCs express TLR4, a transmembrane receptor that recognizes lipopolysaccharide (LPS) of the Gram-negative bacteria [19]. These findings suggest that prostate SMCs might be an unexpected component of inflammatory responses, with this topic in need of further research. Thus, the goal of this work was to characterize the response of SMCs to LPS in a primary culture of prostate stromal cells from normal rat. We performed an ultrastructural morphologic examination as well as the analysis of the cytoskeleton proteins ACTA2, calponin, vimentin, and tenascin, and the innate immunity molecules TLR4, NF-kB, and proinflammatory cytokines.

MATERIALS AND METHODS

Animals

Adult 12-week-old, male rats, Wistar strain, weighing 250–350 g, were housed at the Animal Research Facility of the National University of Córdoba in air-conditioned quarters, under a controlled photoperiod (14-hr light/10-hr darkness) and with free access to commercial rodent food and tap water. Animal care and experiments were conducted following the recommendations of the International Guiding Principles for Biomedical Research Involving Animals, as issued by the Council for International Organization of Medical Sciences (CIOMS).

Prostate Smooth Muscle Cell cultures and Treatment

Prostate specimens were obtained from six Wistar rats per culture. The tissues were minced into small fragments and treated for 30 min with a digestion solution containing 200 U/ml collagenase type IA (Sigma–Aldrich, St. Louis, MO) and 0.05% deoxyribonuclease type I (Sigma) in minimal essential medium SMEM (Sigma). The dispersion was then washed three times with SMEM, with cells being collected by centrifugation for 2 min at 1,000*g* after each wash. Finally, isolated cells were resuspended and adjusted to 1×10^6 cell/ml and cultured in the SMC medium MCDB131 (Sigma) supplemented with 10% heat-inactivated fetal calf serum and 10% horse serum (Gibco, Invitrogen, Carlsbad, CA). These dispersed cells were plated on a six-well culture plate in a humidified incubator at 37°C supplied with 5% CO_2 in air. The medium was replaced daily for 6 days, after finally, was replaced by serum-free medium supplemented with 5 μg/ml insulin, 5 μg/ml transferrin, 5 ng/ml selenite, and 2 ng/ml TGFβ1 (Invitrogen) for 72 hr. During this period, the epithelial cells displayed a poor attachment rate with cellular degeneration being common and the few attached epithelial cells being soon overgrown by the proliferating stromal cells.

To examine the effects of LPS, the SMCs were then incubated in serum-free medium with different doses of LPS (Sigma; 0.1, 1, or 10 μg/ml) for 24 or 48 hr. Then,

to verify the specificity of the LPS actions, SMCs were treated for 1 hr before LPS stimulation with 10 μg/ml of an antibody which recognizes an extracellular domain of TLR4 (Santa Cruz Biotechnology, Santa Cruz, CA).

Electron Microscopy

SMCs were fixed in Karnovsky mixture containing 1.5% (v/v) glutaraldehyde, 4% (w/v) formaldehyde in 0.1 M cacodylate buffer, pH 7.3, plus 7% sucrose for 15 min, before being scrapped from the wells, washed and centrifugated at 1,000*g*. Pellets were maintained in Karnovsky for 2 hr, treated with 1% osmium tetroxide for 1 hr, and dehydrated in a series of graded cold acetones and embedded in Araldite. For ultrastructural studies, 60-nm thin sections were cut with a diamond knife on a Porter-Blum MT2 and JEOL JUM-7 ultramicrotome, and examined with a Zeiss LEO 906E electron microscope.

For ultrastructural immunocytochemistry, SMCs pellets were embedded in acrylic resin (LRWhite; London Resin Corporation, UK) omitting osmium fixation. LRWhite thin sections were mounted on 250-mesh nickel grids and were incubated overnight in a drop of mouse anti-ACTA2 (Novocastra, Newcastle, UK) diluted 1/50, and immunoreactive sites were labeled with 16 nm colloidal gold/anti-mouse IgG complex (Electron Microscopy Sciences, Hatfield, PA). For controls, the primary antibody was replaced with the same dilution of purified mouse IgG (Santa Cruz) or PBS–BSA.

Immunofluorescence

Coverslides containing attached cells were fixed with 4% formaldehyde, permeabilized with 0.25% Triton X-100 in PBS and incubated for 1 hr in 5% PBS–BSA to block non-specific binding. Slides were then incubated overnight at 4°C in a humidified chamber with the following primary antibodies: anti-ACTA2 (1/50 mouse monoclonal; Novocastra), anti-vimentin (1/100 mouse monoclonal; Novocastra), anti-calponin (1/500 mouse monoclonal; Thermo Scientific, Rockford, IL), anti-TLR4 (1/400 polyclonal goat; Santa Cruz), and anti-p65-NF-κB (1/1,000 rabbit antibody polyclonal; Abcam, Cambridge, MA). Afterwards, the slides were washed three times with PBS and further incubated with Alexa 488 anti-mouse, Alexa 594 anti-goat, or Alexa 594 anti-rabbit secondary antibodies (1/1,000 Invitrogen) for 1 hr and mounted using fluoromount containing DAPI. Finally, positive signals were visualized under a Zeiss Axiovert 135 fluorescence microscope.

For double immunostaining, slides were firstly labeled for ACTA2 with Alexa 488 anti-mouse as a secondary antibody, before being washed and incubated with anti-vimentin antibody using the Alexa 594 anti-mouse as explained above.

Western Blotting

For immunoblots, SMCs cultures were homogenized on ice in 120 μl cold PBS containing 1.25% Igepal CA-630, 1 mM EDTA, 2 mM PMSF, 10 μg/ml leupeptin, and 10 μg/ml aprotinin. The lysate was centrifuged at 14,000*g* for 20 min at 4°C to pellet the Igepal CA-630-insoluble material, and the supernatant was stored in aliquots frozen at −70°C until required. Total protein concentration was measured with a Bio-Rad kit (Bio-Rad Laboratories, Hercules, CA), and denatured protein samples (30 μg/lane) were separated on 12% SDS–polyacrylamide gel and blotted onto a Hybond-C membrane (Amersham Pharmacia, Buckinghamshire, UK). To assess the corresponding molecular weight, Full Range Rainbow Molecular Weight Marker (Amersham Pharmacia) was used, with incubation steps beingmeasured by commercially performed in 5% defatted dry milk in PBS/0.1% Tween 20. Membranes were rinsed and incubated for 3 hr with a goat polyclonal antibody diluted 1/400 (which recognizes TLR4 [Santa Cruz]), 1/1,000 rabbit anti-CD14 (Santa Cruz), 1/200 mouse anti-ACTA2 (Novocastra), 1/300 mouse anti-Vimentin (Novocastra), 1/500 mouse anti-calponin (Thermo Scientific), or 1/500 goat anti-tenascin-C (Santa Cruz). After washing, the blots were incubated with a peroxidase-conjugated (HRP) bovine anti-goat (Santa Cruz), goat anti-rabbit (Santa Cruz), or goat anti-mouse (Jackson Immunoresearch, West Grove, PA) secondary antibody, and exposed with ECL Western blot detection reagents (Amersham Pharmacia) following the manufacturer's instructions. Emitted light was captured on Hyperfilm (Amersham Pharmacia) and densitometry analysis was performed by applying Scion Image software (V. beta 4.0.2; Scion Image Corp., Frederick, MD). The relative expression was compared among different treatments by taking the control group value as a reference. The expression of ACTB (1/5,000; monoclonal anti-βactin; Sigma) was used as an internal control to confirm equivalent total protein loading.

ELISA

In order to quantify TNFα and IL6 secretion by SMCs after LPS stimulation, 1ml medium was collected from the plates, centrifuged at 4°C, 1,400 rpm for 15 min and stored at −20°C until the day of the assay. Secretion was measured by commercially available sandwich ELISA kits (eBioscience, San Diego, CA for TNFα and BD Biosciences, Franklin Lakes, NJ for IL6), following the manufactureŕs instructions.

Proliferation Assay

SMCs were stimulated with LPS for 24 hr, with BrdU (3 mg/ml) being added to the culture medium 3 hr before finishing protocols. The cells attached to the coverslips were fixed with 4% formaldehyde in PBS for 30 min at room temperature, washed in PBS, and permeabilized with 0.5% Triton X-100 for 10 min. Nonspecific immunoreactivity was blocked with 1% PBS–BSA for 30 min at RT, and the cells were incubated overnight with a monoclonal antibody against BrdU (Amersham Pharmacia) at 4°C in a wet chamber. After being washed in PBS, the cells were incubated with biotinylated anti-mouse IgG diluted 1/100 (GE Healthcare, Buenos Aires, Argentina). The coverslips were washed again with PBS, and incubated with the avidin–biotinperoxidase complex (ABC; Vector; Burlingame). The immunoreactivity for BrdU was visualized with 3,3-diaminobenzidine tetrahydrochloride (DAB) as a chromogen. A total of 1,000 immunoreactive cells were examined by light microscopy in randomly chosen fields of each glass slide, in order to establish the percentage of BrdU immunoreactive cells. Three slides were analyzed for each group, derived from the same cell preparations. Experiments were replicated at least three times with separate batches of cell preparations.

Statistical Analysis

Data from more than two groups were examined using analysis of variance with Tukey's as post-test. Statistical testing and calculation of Western blot data were performed using the InStat V2.05 software from GraphPad, Inc.

RESULTS

TLR4 Is Present in Prostate SMCs and Increases After LPS Stimulation

As a prerequisite for analyzing the effects of LPS on SMCs, we first examined the presence of its receptor TLR4. As shown in Figure 1, immunofluorescence produced a moderate signal for TLR4 in control cells. On the other hand, LPS elicited an increase in TLR4 expression in SMCs in a dose- and time-dependent manner as evaluated by Western blot (Fig. 1A,B). These last results were confirmed by immunofluorescence, which indicated a rise in the intensity of TLR4 expression in stimulated cells (Fig. 1C).

The coreceptor CD14, an important adapter molecule of the TLR4 signaling pathway, was also found to be expressed in prostate SMCs. However, no changes in this expression were detected either at 24 or 48 hr after LPS treatment (Fig. 1A).

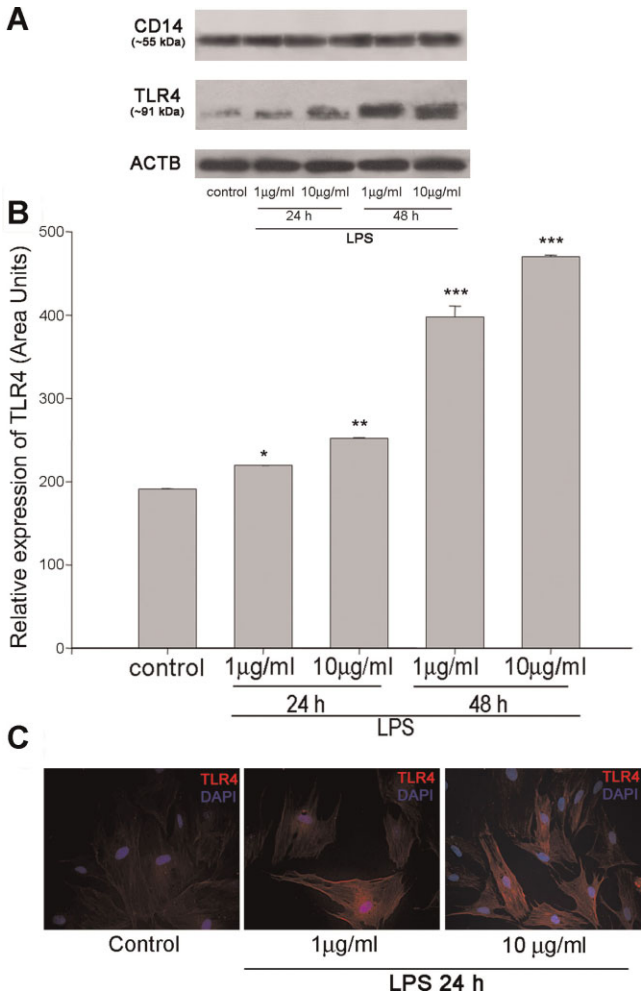

Fig. 1. TLR4 expression in SMCs by Western blot (**A**,**B**) and immunofluorescence (**C**). SMCs express TLR4 in control conditions (A); after LPS treatment there was a significant increase of TLR4 expression, which was dose- and time-dependent as evaluated by densitometric analysis (B), with CDI4 expression not showing any changes after LPS stimulation (A). Immunofluorescence also shows higher TLR4 staining after LPS, mainly when a I0 μg/ml concentration was applied (C). Nuclei were counterstained with DAPI. The Western blot values were normalized with ACTB expression and represent the mean ± SE from five independent protocols. * versus control $P < 0.05$, ** versus control $P < 0.0I$; *** versus control $P < 0.00I$ ANOVA-Tukey.

LPS Effects on SMC Phenotype

The phenotype of SMCs was determined by analyzing ultrastructural features by electron microscopy, and evaluating the stromal cell differentiation markers ACTA2, calponin, and vimentin. Whereas ACTA2 and calponin are early and late markers of SMCs, respectively, vimentin is a mesenchymal cell intermediate filament that is expressed on fibroblasts. Expression of ACTA2 and vimentin without calponin has been

previously shown to indicate a myofibroblastic-like phenotype [20].

Unstimulated SMCs displayed a homogeneous cytoplasmic compartment, with a large contractile apparatus and scarce organelles (Fig. 2A). Immunogold labeling revealed that ACTA2 was widespread in the whole cytoplasm at ultrastructural level (Fig. 2D), with immunofluorescence for the stromal cell differentiation markers demonstrating that the SMC phenotype represented 95% of total cells, expressing high levels of ACTA2 and calponin, but weak levels of vimentin (Fig. 3).

After treatment with 1 μg/ml of LPS, the SMCs showed numerous mitochondria and dilated cisterns of RER with secretory content and well-developed Golgi complexes (Fig. 2B). These findings were more notable in cultures stimulated with 10 μg/ml of LPS (Fig. 2C). The immunogold labeling demonstrated a decrease in ACTA2, which was confined to the peripheral regions (Fig. 2E,F), while most cytoplasmic areas appeared to be full of proteinpoyetic organelles. Immunofluorescence confirmed the disorganization of the ACTA2 cytoskeleton. In controls, labeling delineated typical stress fibers, while after 24 hr of LPS, cells exhibiting ''patches'' with intense ACTA2 expression and discontinuous stress fibers were frequently observed (Fig. 3D). At 48-hr post-stimulation, cells with lower ACTA2 levels predominated. In addition, LPS challenge induced an increase in vimentin immunofluorescence but a decrease in calponin expression compared to control cells (Fig. 3D). In order to corroborate the SMC phenotype after LPS treatment, we performed a double immunofluorescence for ACTA2 and vimentin. Unstimulated SMCs were only positive for ACTA2 (Fig. 4A), while cells stimulated with 1 μg/ml of LPS expressed both differentiation markers at 24 hr, with this being more remarkable at 48 hr after LPS treatment (Fig. 4B,C).

Changes in differentiation marker levels were corroborated by Western blot. LPS challenge significantly increased vimentin expression at 24 hr in a dose-dependent manner (Fig. 3C), whereas ACTA2 and calponin were significantly decreased for a 1 μg/ml dose (Fig. 3A,B). After 48 hr of LPS stimulation, ACTA2 and calponin expression decreased even further compared to 24 hr, whereas the levels of vimentin increased (Fig. 3A–C). Moreover, LPS induced a rise in tenascin-C, a key glycoprotein of the extracellular matrix in reactive stroma [20]. This finding was observed at 24 hr after 1 μg/ml, with this increase being more remarkable after 10 μg/ml of LPS (Fig. 5).

In order to investigate if changes in the SMC phenotype induced by LPS were mediated by interaction with TLR4, we applied an anti-TLR4 antibody before

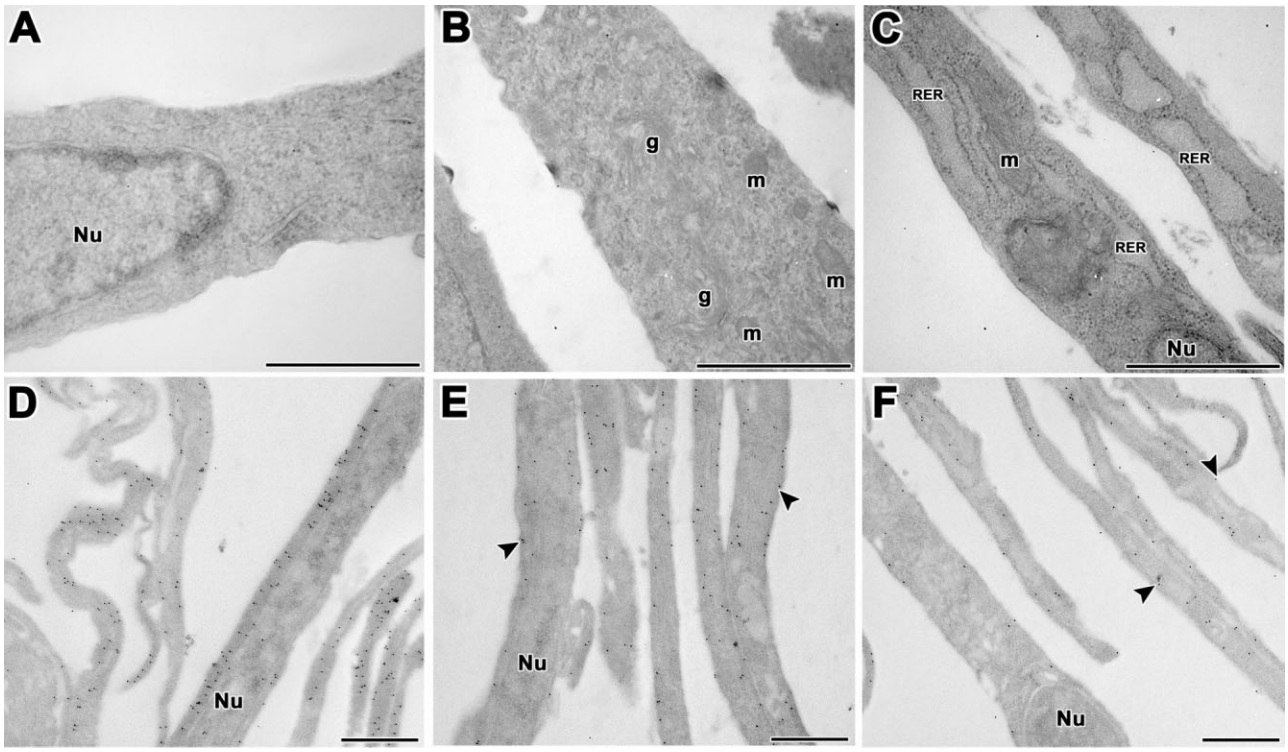

Fig. 2. Ultrastructure of SMCs included in plastic resins. Control cells show scarce organelles (**A**). After LPS, cells have signs of cell activation as numerous mitochondria (m), well-developed Golgi complexes (g), and dilated cisterns of RER with secretory content (**B**,**C**). Immunogold reveals intense ACTA2 labeling in control cells (**D**), while after LPS it diminished markedly (arrowheads in **E** and **F**). Nu: nucleus. Bar: 1 μm.

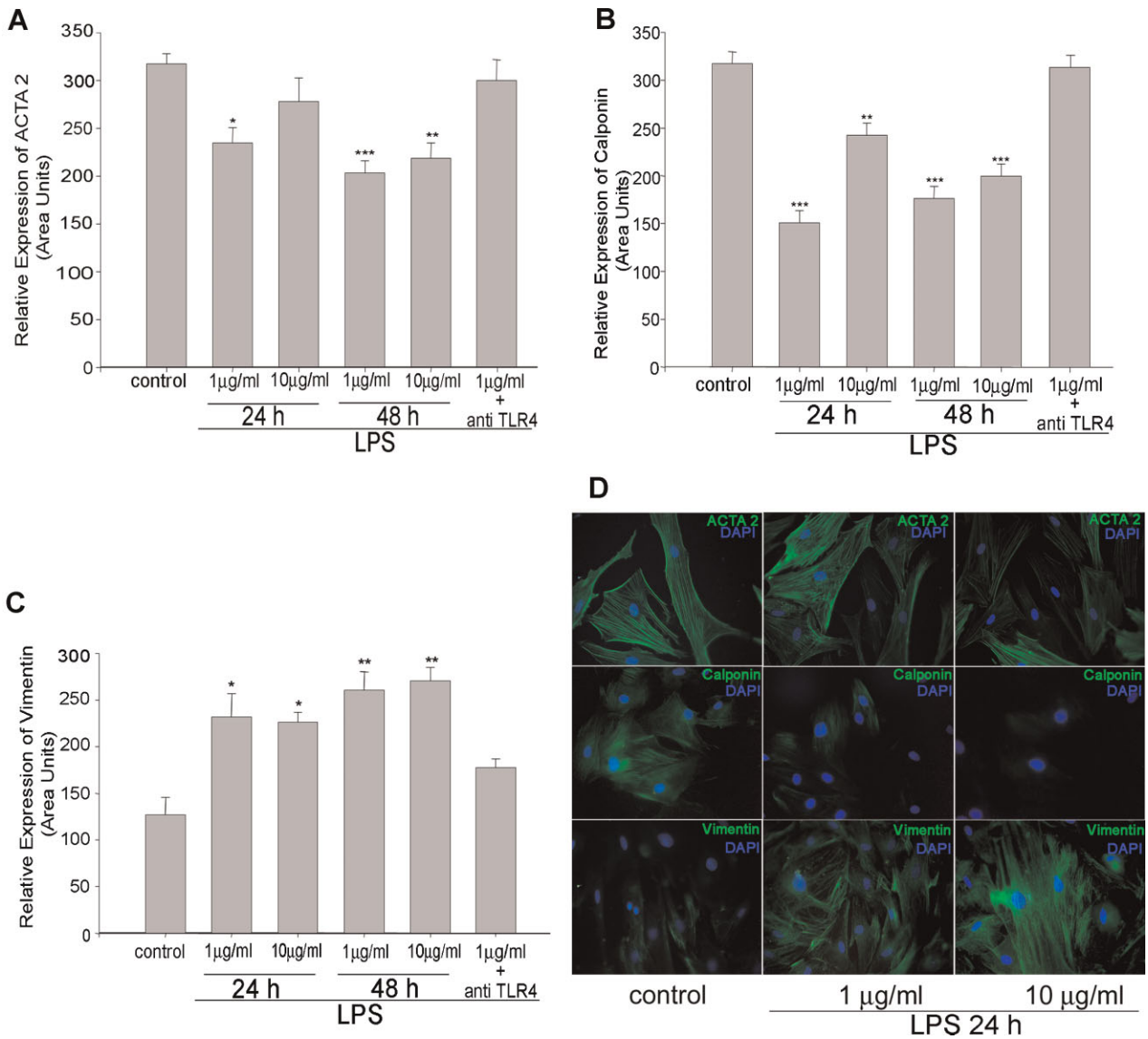

Fig. 3. Stromal cell differentiation markers by Western blot (**A**–**C**) and immunofluorescence (**D**). A significant decrease of the ACTA2 and calponin expressions occurred at 24 hr, which intensified at 48 hr after LPS as evidenced by the densitometric analysis (A,B). Meanwhile, vimentin content showed a dose-dependent increase after LPS treatment (C). For all differentiation markers, changes induced by LPS were avoided when an anti-TLR4 antibody was applied before stimulation. Immunofluorescence shows that control SMCs express ACTA2 and calponin, but are negative for vimentin (D). After an LPS stimulation of 24 hr, vimentin expression was induced at the lower concentration and intensified at 10 µg/ml. A reduction in the calponin content was evident even at the lower dose. ACTA2 labeling shows patches and disorganization of stress fibers, at 1 µg/ml of LPS, and an evident reduction at 10 µg/ml (D). Nuclei were counterstained with DAPI. The Western blot values were normalized with ACTB expression, and represent the mean of the cultures per group obtained from three independent protocols. * versus control $P < 0.05$, ** versus control $P < 0.01$, *** versus control, $P < 0.001$. ANOVA-Tukey.

LPS challenge. The use of this antibody prevented any alterations in the differentiation markers ACTA2, vimentin, or calponin (Fig. 3).

LPS Induces NF-κB Activation and Upregulation of Proinflammatory Mediators

It is well-known that TLR4 activation produces a cascade of downstream signals that finally leads the transcription factor NF-κB to translocate to the nucleus, thereby activating a large number of genes related to the inflammatory response. We therefore decided to investigate the nuclear localization of NF-κB in SMCs as a sign of activation after LPS stimulation. For this purpose, SMCs were subjected to LPS challenge with 1 or 10 µg/ml for 10, 30, and 120 min, and NF-κB expression was revealed by immunostaining the p65 subunit under fluorescent microscopy. Control cells exhibited a

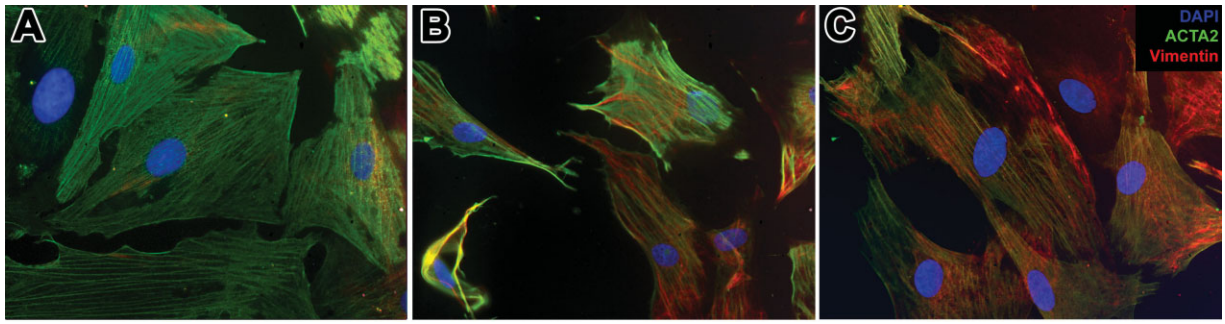

Fig. 4. Co-expression of ACTA 2 and vimentin in myofibroblast-like cells after LPS treatment. Control SMCs express mainly ACTA2 (**A**), while in cells treated with 1 μg/ml of LPS at 24 hr (**B**), the merged image shows vimentin (red) and ACTA2 (green), with ACTA2 predominating. After 48 hr of treatment (**C**), co-expression is maintained with predominant expression of vimentin. Nuclei were stained with DAPI (blue).

basal number of cells with nuclear NF-κB (1.75% of cells). In contrast, LPS-treated SMCs showed a notable increase in the number of cells exhibiting nuclear NF-κB, with 34.4% of cells observed at 10 min and 27% of cells at 30 min. After 120 min, the number of SMCs displaying NF-κB nuclear translocation was reduced to 5% of the total cell population (Fig. 6).

We also examined the secretion of cytokines as molecules triggered by TLR4 activation. The levels of TNFα and IL6 were measured by ELISA in a supernatant of SMCs incubated with 1 and 10 μg/ml of LPS for 24 or 48 hr. Both concentrations of LPS induced a significant increase in IL6 secretion after 24 hr with even higher levels at 48 hr (Fig. 7B). The TNFα levels also increased, but only after 48 hr of LPS exposition (Fig. 7A).

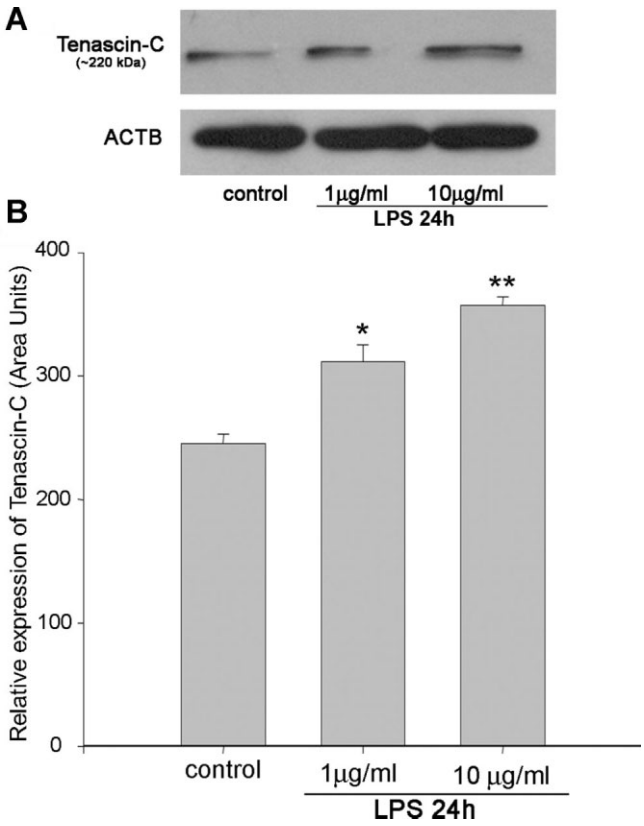

Fig. 5. Tenascin-C expression in SMCs. (**A**) Relative amounts of tenascin-C were measured by densitometric analysis of Western blot (**B**), which demonstrated a significant increase in tenascin expression after LPS stimulation in comparison with controls. The values represent tenascin levels after normalization with ACTB expression in SMC. * versus control $P < 0.05$, ** versus control $P < 0.01$.

LPS Promotes Cellular Proliferation

In addition to phenotypic changes, LPS treatment elicited a significant increase in BrdU-positive cells, with higher differences being found at the dose of 1 μg/ml (fourfold compared to control; Fig. 8), indicating the induction of proliferative activity of SMCs after LPS stimulation.

DISCUSSION

For many years, studies dealing with prostate research were mainly focused on epithelial cells. However, the prostatic stromal compartment has acquired more attention over the last decade, with its characterization and behavior being important in order to understand its role in prostatic disorders. Here, we demonstrate that prostate SMCs are capable of responding to LPS in vitro by changing their contractile phenotype toward a secretory profile. This altered phenotype exhibited a significant loss of ACTA2 and calponin while increasing vimentin content, which is consistent with myofibroblastic-like cells. Furthermore, the TLR4 signaling pathway and NF-κB translocation were involved in this reaction as well as in the cytokine secretion by SMCs after LPS challenge.

The process of SMC dedifferentiation and acquisition of a secretory phenotype has been previously described for other inflammatory conditions of many organs, especially in the early development of

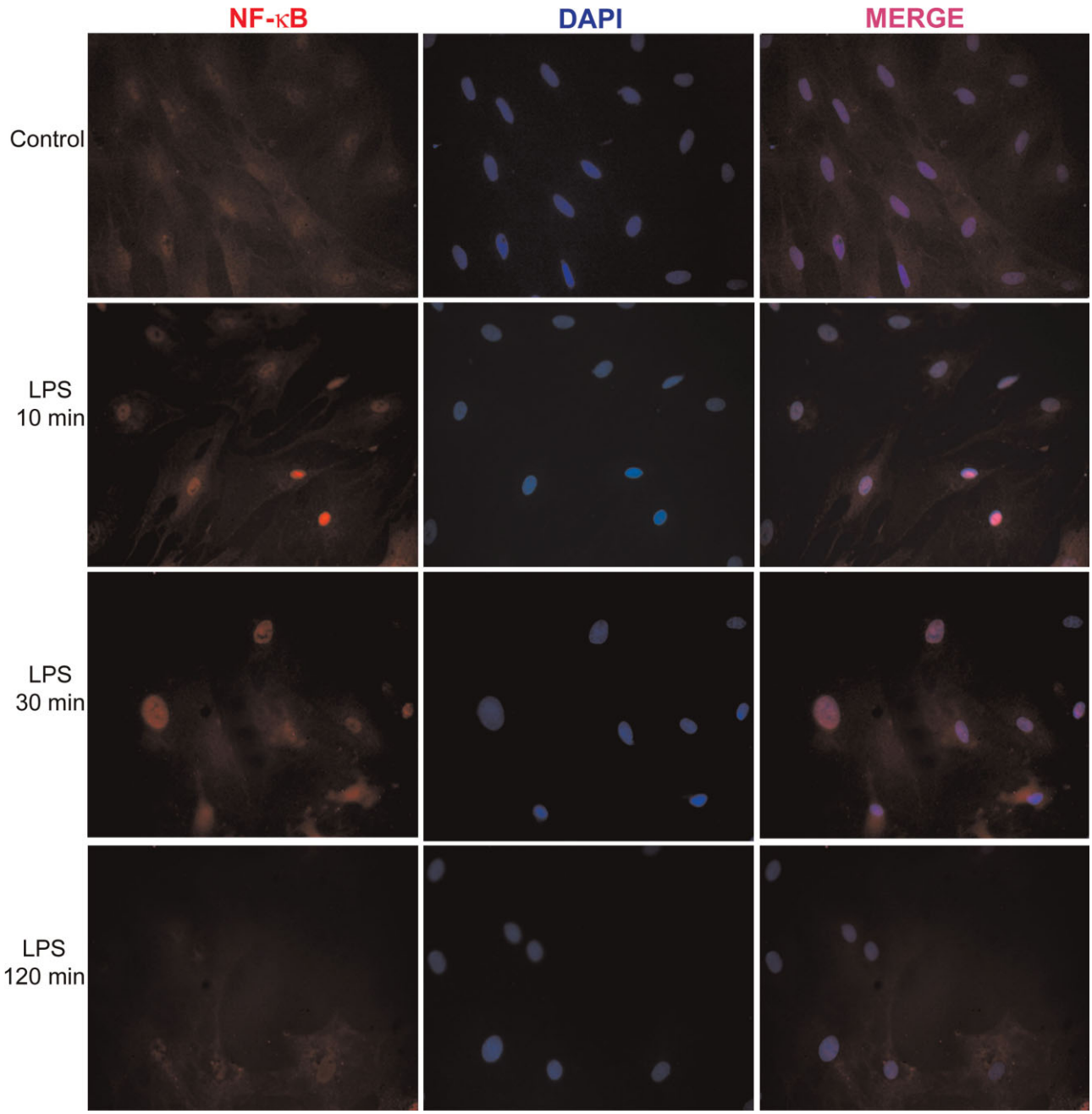

Fig. 6. Nuclear translocation of NF-*k*B after LPS. SMC were cultured with LPS (1 μg/ml) for 10, 30, or 120 min. NF-κB nuclear localization resulted in colocalization of p65 (red) and DAPI (blue) signals, producing purple fluorescence. The experiment was performed three times, and the pictures correspond to a representative field for each time period studied.

atherosclerosis [21] and in the progression of asthma [14]. However, in the case of the prostate, the dedifferentiation of SMCs has been mainly investigated in cancer and BPH, with dedifferentiated SMCs with loss of myosin, desmin, and laminin found to be localized adjacent to precancerous sites and associated to cancer development [8]. Moreover, the stromal compartment accompanying prostatic intraepithelial neoplasia and prostate cancer creates a wound repair-type process called reactive stroma [20,22], in which the cellular composition is severely altered from physiological SMCs to a myofibroblastic phenotype. This new cellular pattern is more sensitive to the microenvironment, being able to proliferate and produce matrix and growth factors. Thus, myofibroblasts forming reactive stroma are important elements in the progression of prostate cancer [11]. Nevertheless, the alterations of the prostatic stromal phenotype in other inflammatory

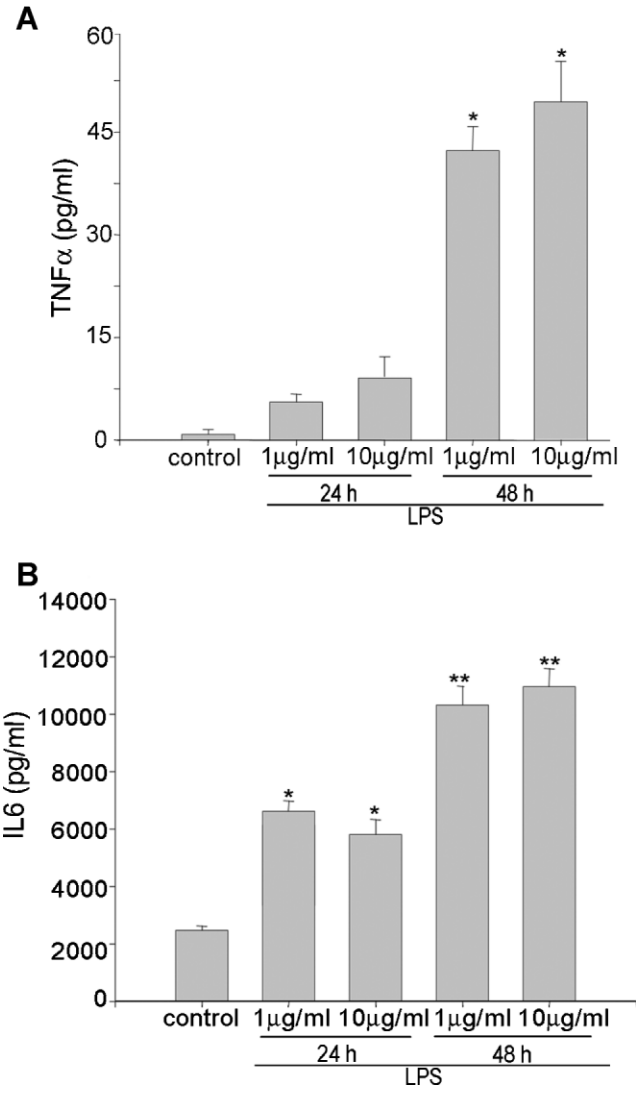

Fig. 7. Cytokine production in SMCs stimulated by LPS. IL6 and TNFα levels were measured by ELISA in supernatants. TNFα was induced only after 48 hr of LPS treatment (**A**), while IL6 showed a marked increase at both doses and the times evaluated (**B**). Data refer to mean ± SE from three separate experiments. * versus control, $P < 0.05$, ** versus control, $P < 0.01$. ANOVA-Tukey.

pathologies such as prostatitis have not yet been fully explored.

Our group previously has described SMCs reacting to bacterial inflammation, initially with hypertrophy and then by acquiring a secretory phenotype in a rat model of acute prostatitis [18]. In the present study, we have confirmed that SMCs respond specifically to bacterial LPS, with important changes occurring in their fine structure. SMCs were found to increase proteinpoietic organelles and mitochondria while decreasing contractile filaments, indicating the loss of their normal contractile phenotype after LPS treatment. Furthermore, LPS induced cellular proliferation and

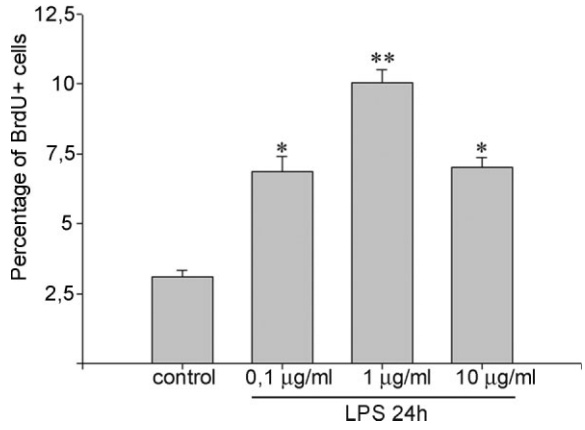

Fig. 8. Analysis of proliferation expressed as percentage of BrdU positive cells. Proliferation was induced with the three LPS doses applied. * versus control $P < 0.05$; ** versus control, $P < 0.01$, ANOVA-Tukey.

expression of vimentin, with these cells co-expressing ACTA2 and vimentin, thereby suggesting a myofibroblastic-like phenotype. A similar process was described for vascular SMCs during the progression of atherosclerosis, where proinflammatory cytokines appeared to be responsible for the transition from a contractile/quiescent phenotype to a secretory proliferative one as observed in these cells [23]. In asthma, recent evidence indicates that SMCs secrete inflammatory mediators, thus playing a role in orchestrating and perpetuating airway inflammation and fibrosis [24].

There are many reports about SMCs being metabolically dynamic cells in addition to their primary function in contraction [25]. Indeed, they are able to recognize pathogen patterns through TLRs and to respond secreting cytokines, chemokines, growth factors, and other immune mediators when stimulated by specific TLR ligands. These findings have been demonstrated at many sites, including the respiratory [26], gastrointestinal [27], and vascular systems [16]. In the prostate, we previously showed the presence of TLR4 in SMCs, whose expression was increased after acute bacterial prostatitis and following castration [19]. Moreover, a recent report documented that SMCs from BPH patients express all types of TLRs and harbor the capacity to secrete IL8, CXCL10, and IL6 after proinflammatory stimuli. That work also suggested that prostate SMCs could act as non-professional antigen-presenting cells [7]. In addition, the present study demonstrates that LPS upregulates TLR4, inducing nuclear translocation of NF-κB and the subsequent secretion of TNFα and IL6 in primary SMC cultures from normal rat prostate, indicating a key role for SMCs in the innate immune response against pathogens.

Since SMCs have been described to have a pivotal function in the maintenance of stromal–epithelial interactions [28], their dedifferentiation and the loss

of normal activity after inflammatory stimuli may induce or contribute to proliferative pathologies such as prostate cancer and BPH [29]. For BPH in particular, IL6 production by stromal cells has been described as a potential autocrine growth factor with a proliferative effect [30], which is consistent with the IL6 secretion found in this work and the rise in proliferation. Certain inflammatory mediators have been attributed to be able to change the phenotype of prostatic stromal cells. For instance, Schauer et al. [31] demonstrated that human prostatic fibroblasts acquire a myofibroblastic phenotype after IL8 treatment, indicating that this molecule could be implicated in the maintenance of reactive stroma in BPH. However, our report is the first to show that LPS can specifically induce SMC cultures to adopt a myofibroblastic phenotype. Hence, in an in vivo scenario, the myofibrablastic pattern occurring in many prostatic diseases may be sustained not only by proinflammatory cytokines and growth factors but also by the direct effects of pathogen compounds on stromal cells.

In the prostate gland, our findings indicate that, even in culture, prostatic SMCs are capable of responding to proinflammatory LPS in the absence of contact with epithelial or professional immune cells. Thus, SMCs play a role in prostate gland response to bacterial infection by releasing mediators to eliminate microorganisms as well as sustaining and amplifying the inflammatory profile observed in experimental prostatitis [18]. However, the dedifferentiation of SMCs in response to pathogen molecules alters the stromal–epithelial interactions, thus compromising the homeostasis of the prostate gland. Consequently, prostate SMCs may contribute at the same time to the pathophysiology of inflammatory diseases.

ACKNOWLEDGMENTS

We thank Dr. Bryan Eyden for his clear concepts on myofibroblastic-like cells. We gratefully acknowledge the excellent technical assistance of Mercedes Guevara, Elena Pereyra, Christian Giacomelli, and Lucía Artino. We are also indebted to Claudia Sotomayor (CIBICI-CONICET) for the training in ELISA and Cecilia Sampedro for help us in fluorescence imaging. Thanks are due to Team-18 and C7 for their constant advice. We would also like to thank native speaker Dr. Paul Hobson for revision of the manuscript.

REFERENCES

1. Flickinger CJ. The fine structure of the interstitial tissue of the rat prostate. Am J Anat 1972;134(1):107–125.
2. Thomson AA, Cunha GR, Marker PC. Prostate development and pathogenesis. Differentiation 2008;76(6):559–564.
3. Boesch ST, Corvin S, Zhang J, Rogatsch H, Bartsch G, Klocker H. Modulation of the differentiation status of cultured prostatic smooth muscle cells by an alpha1-adrenergic receptor antagonist. Prostate 1999;39(4):226–233.
4. Wu Q, Shi J, Chen L, Wang CY, Park I, Lee C, Zhang J. Regulation of proliferation and differentiation of prostatic stromal cells by oestradiol through prostatic epithelial cells in a paracrine manner. BJU Int 2008;101(4):497–502.
5. Kassen A, Sutkowski DM, Ahn H, Sensibar JA, Kozlowski JM, Lee C. Stromal cells of the human prostate: Initial isolation and characterization. Prostate 1996;28(2):89–97.
6. Shapiro E, Becich MJ, Hartanto V, Lepor H. The relative proportion of stromal and epithelial hyperplasia is related to the development of symptomatic benign prostate hyperplasia. J Urol 1992;147(5):1293–1297.
7. Penna G, Fibbi B, Amuchastegui S, Cossetti C, Aquilano F, Laverny G, Gacci M, Crescioli C, Maggi M, Adorini L. Human benign prostatic hyperplasia stromal cells as inducers and targets of chronic immuno-mediated inflammation. J Immunol 2009;182(7):4056–4064.
8. Wong YC, Tam NN. Dedifferentiation of stromal smooth muscle as a factor in prostate carcinogenesis. Differentiation 2002; 70(9–10):633–645.
9. Ayala G, Tuxhorn JA, Wheeler TM, Frolov A, Scardino PT, Ohori M, Wheeler M, Spitler J, Rowley DR. Reactive stroma as a predictor of biochemical-free recurrence in prostate cancer. Clin Cancer Res 2003;9(13):4792–4801.
10. Sappino AP, Schurch W, Gabbiani G. Differentiation repertoire of fibroblastic cells: Expression of cytoskeletal proteins as marker of phenotypic modulations. Lab Invest 1990;63(2):144–161.
11. Tuxhorn JA, Ayala GE, Rowley DR. Reactive stroma in prostate cancer progression. J Urol 2001;166(6):2472–2483.
12. Fulmer BR, Turner TT. Effect of inflammation on prostatic protein synthesis and luminal secretion in vivo. J Urol 1999; 162(1):248–253.
13. Gatti G, Rivero V, Motrich RD, Maccioni M. Prostate epithelial cells can act as early sensors of infection by up-regulating TLR4 expression and proinflammatory mediators upon LPS stimulation. J Leukoc Biol 2006;79(5):989–998.
14. Borger P, Tamm M, Black JL, Roth M. Asthma: Is it due to an abnormal airway smooth muscle cell? Am J Respir Crit Care Med 2006;174(4):367–372.
15. van Oostrom O, Fledderus JO, de Kleijn D, Pasterkamp G, Verhaar MC. Smooth muscle progenitor cells: Friend or foe in vascular disease? Curr Stem Cell Res Ther 2009;4(2):131–140.
16. Heo SK, Yun HJ, Noh EK, Park WH, Park SD. LPS induces inflammatory responses in human aortic vascular smooth muscle cells via Toll-like receptor 4 expression and nitric oxide production. Immunol Lett 2008;120(1–2):57–64.
17. Singer CA, Salinthone S, Baker KJ, Gerthoffer WT. Synthesis of immune modulators by smooth muscles. Bioessays 2004;26(6): 646–655.
18. Quintar AA, Doll A, Leimgruber C, Palmeri CM, Roth FD, Maccioni M, Maldonado CA. Acute inflammation promotes early cellular stimulation of the epithelial and stromal compartments of the rat prostate. Prostate 2010;70(11):1153–1165.
19. Quintar AA, Roth FD, De Paul AL, Aoki A, Maldonado CA. Toll-like receptor 4 in rat prostate: Modulation by testosterone and acute bacterial infection in epithelial and stromal cells. Biol Reprod 2006;75(5):664–672.
20. Tuxhorn JA, Ayala GE, Smith MJ, Smith VC, Dang TD, Rowley DR. Reactive stroma in human prostate cancer: Induction of

myofibroblast phenotype and extracellular matrix remodeling. Clin Cancer Res 2002;8(9):2912–2923.

21. Denger S, Jahn L, Wende P, Watson L, Gerber SH, Kubler W, Kreuzer J. Expression of monocyte chemoattractant protein-1 cDNA in vascular smooth muscle cells: Induction of the synthetic phenotype: A possible clue to SMC differentiation in the process of atherogenesis. Atherosclerosis 1999;144(1):15–23.
22. Desmouliere A, Guyot C, Gabbiani G. The stroma reaction myofibroblast: A key player in the control of tumor cell behavior. Int J Dev Biol 2004;48(5–6):509–517.
23. Clement N, Glorian M, Raymondjean M, Andreani M, Limon I. PGE2 amplifies the effects of IL-1beta on vascular smooth muscle cell de-differentiation: A consequence of the versatility of PGE2 receptors 3 due to the emerging expression of adenylyl cyclase 8. J Cell Physiol 2006;208(3):495–505.
24. Tliba O, Panettieri RA Regulation of inflammation by airway smooth muscle. Curr Allergy Asthma Rep 2008;8(3):262–268.
25. Gerthoffer WT, Singer CA. Secretory functions of smooth muscle: Cytokines and growth factors. Mol Interv 2002;2(7): 447–456.
26. Diamond G, Legarda D, Ryan LK. The innate immune response of the respiratory epithelium. Immunol Rev 2000;173:27–38.
27. Scirocco A, Matarrese P, Petitta C, Cicenia A, Ascione B, Mannironi C, Ammoscato F, Cardi M, Fanello G, Guarino MP, Malorni W, Severi C. Exposure of Toll-like receptors 4 to bacterial lipopolysaccharide (LPS) impairs human colonic smooth muscle cell function. J Cell Physiol 2010;223(2):442–450.
28. Hayward SW, Cunha GR, Dahiya R. Normal development and carcinogenesis of the prostate. A unifying hypothesis. Ann N Y Acad Sci 1996;784:50–62.
29. Taboga SR, Scortegagna E, Siviero MP, Carvalho HF. Anatomy of smooth muscle cells in nonmalignant and malignant human prostate tissue. Anat Rec (Hoboken) 2008;291(9):1115–1123.
30. Fibbi B, Penna G, Morelli A, Adorini L, Maggi M. Chronic inflammation in the pathogenesis of benign prostatic hyperplasia. Int J Androl 2010;33(3):475–488.
31. Schauer IG, Ressler SJ, Tuxhorn JA, Dang TD, Rowley DR. Elevated epithelial expression of interleukin-8 correlates with myofibroblast reactive stroma in benign prostatic hyperplasia. Urology 2008;72(1):205–213.